Improved Fatigue Resistance of Al-Zn-Mg-Cu (7075) Alloys Through Thermomechanical Processing

F. OSTERMANN

To decrease the accumulation of damage during long-life low-stress cyclic loading, microstructures must accommodate inelastic deformation by homogeneous or "dispersed" slip rather than by localized slip concentrations. In age-hardening aluminum alloys this requirement can be met by introducing a dense and uniform dislocation forest through suitable thermo-mechanical treatments. Such a treatment was developed for Al-Zn-Mg-Cu (7075) alloys, involving a process cycle of solution annealing, partial aging, mechanical working and final aging. The fatigue properties (*S-N* curves) of commercial and high-purity 7075TMT are compared with conventional 7075-T651 properties; with zero mean stress the alternating stress to cause failure in 10^7 cycles is more than 25 pct higher for commercial-purity 7075TMT and almost 50 pct higher for high-purity 7075TMT. The results emphasize the importance of microstructural control when high fatigue resistance is required.

A qualitative, yet detailed, picture has emerged from the efforts of many investigators[1-16] describing various microstructural changes associated with the accumulation of fatigue damage in age-hardened aluminum alloys. While one might desire a more quantitative correlation between microstructural properties and the fatigue processes, it is worthwhile to attempt to synthesize microstructures which should be more resistant to fatigue damage using the presently available information. In a recent review of thermomechanical processing and fatigue of age-hardened aluminum alloys Ostermann and Reimann[17] proposed requirements for microstructures of age-hardened aluminum alloys resistant to the accumulation of fatigue damage in the high-cycle fatigue regime.

The principal requirement for high-cycle fatigue resistance is the ability of the alloy to deform by homogeneous or dispersed slip rather than by slip concentrating in narrow, isolated bands. Homogeneous deformation of age-hardened alloys requires a homogeneous microstructure, *i.e.* absence of strain-concentrating nonmetallic and intermetallic inclusions, and precipitate-free zones. The precipitate-strengthened matrix must also be stable during cyclic loading and resist reversion and overaging of the second-phase particles due to dislocation motion and other slip induced lattice defects. Deformation of such an ideal, homogeneous alloy structure, however, will not be necessarily homogeneous, since the initiation of slip in a highly precipitation-strengthened matrix is quite difficult and slip bands, once they are formed, remain narrow[18-20] and thereby localize further deformation during cyclic loading.

Thermomechanical treatment (TMT) of age-hardened alloys[17] offers the possibility of dispersing the slip and broadening slip bands by introducing abundant slip initation sites through mechanical working. For this purpose thermomechanical treatments must be aimed at generating a uniform dislocation distribution which is strongly locked by precipitate phases to resist localized softening. Properly applied TMT will also provide a more homogeneous microstructure as well as improvements of strength without severe loss of ductility.[17] Such a treatment was developed recently for the high-strength 7075 aluminum alloy.[21] The results of fatigue tests on 7075TMT aluminum are reported here. While the bulk of data were obtained on commercial-purity 7075 bars, some data are presented on high-purity 7075 in order to determine the effects of inclusions on the fatigue behavior.

MATERIAL

Commercial, rolled bar stock was tested in the as-received T651 condition to provide base-line data. The chemical composition of this alloy, designated C7075, is given in Table I along with standard composition limits. Also given in Table I is the composition of the high-purity X7075 alloy, which was vacuum melted from high-purity components, chill cast into a 3.5 in. diam iron mold, homogenized at 870°F (465°C) for 20 hr, and annealed at 775°F (413°C). Reduction of the ingot to bar stock was accomplished by extrusion at 800°F (427°C) followed by hot and cold swaging in order to achieve a recrystallized structure similar to that of the rolled, commercial alloy.

A thermomechanical treatment was given both com-

Table I. Chemical Analysis of Experimental Materials and Standard Composition Limits of Aluminum Alloy 7075 (in Wt Pct)

Elements	Limits	C7075	X7075
Aluminum	Remainder	Remainder	Remainder
Copper	1.20 to 2.00	1.56	1.59
Magnesium	2.10 to 2.90	2.42	2.64
Zinc	5.10 to 6.10	5.53	5.53
Silicon	0.50 max	0.11	<0.01
Manganese	0.30 max	0.04	<0.01
Chromium	0.18 to 0.40	0.19	0.29
Iron	0.70 max	0.26	0.01
Titanium	0.20 max	0.05	0.19
Others: Each	0.05 max	<0.05	<0.05
Total	0.15 max	<0.15	<0.15

F. OSTERMANN, formerly with Air Force Materials Laboratory, Wright-Patterson Air Force Base, Ohio, is now with Leichtmetall-Forschungsinstitut, Vereinigte Aluminum-Werke A.G., Bonn, Germany.

Manuscript submitted February 12, 1971.

mercial and high-purity bars by solution annealing at 860°F (460°C) for 1 hr, water quenching, aging at 212°F (100°C) for 1 hr, swaging at room temperature, and aging at 248°F (120°C) for 16 hr. The commercial alloy, C7075TMT, was reduced 30 pct in cross-section, whereas the high-purity alloy, X7075TMT, was swaged only 10 pct because of specimen size limitations.

MICROSTRUCTURES

The micrographs in Figs. 1 and 2 are of the commercial and high-purity alloys, respectively. The optical microstructure of the commercial material is representative of both the T651 and TMT conditions save for the appearance of a subgrain structure in the

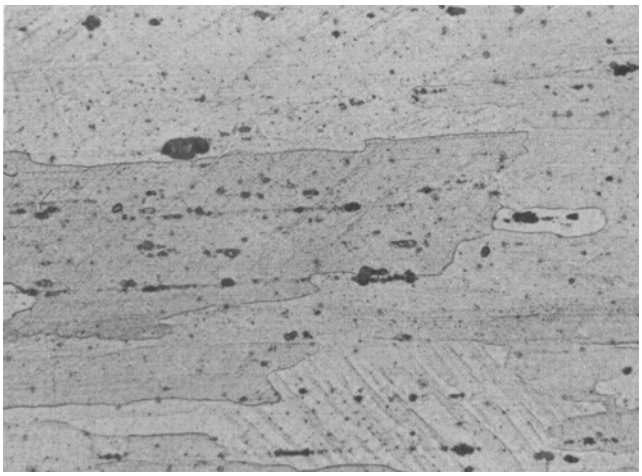

Fig. 1—Grain structure and inclusion particles of commercial aluminum alloy C7075TMT. Keller's etch. Magnification 209 times.

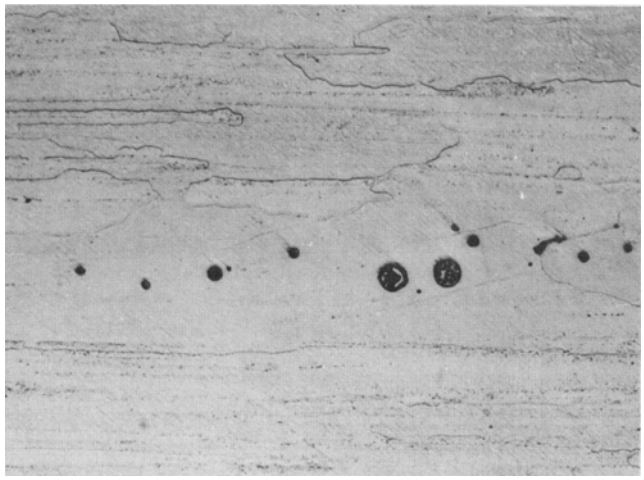

Fig. 2—Grain structure and inclusion particles of high-purity aluminum alloy X7075TMT. Keller's etch. Magnification 209 times.

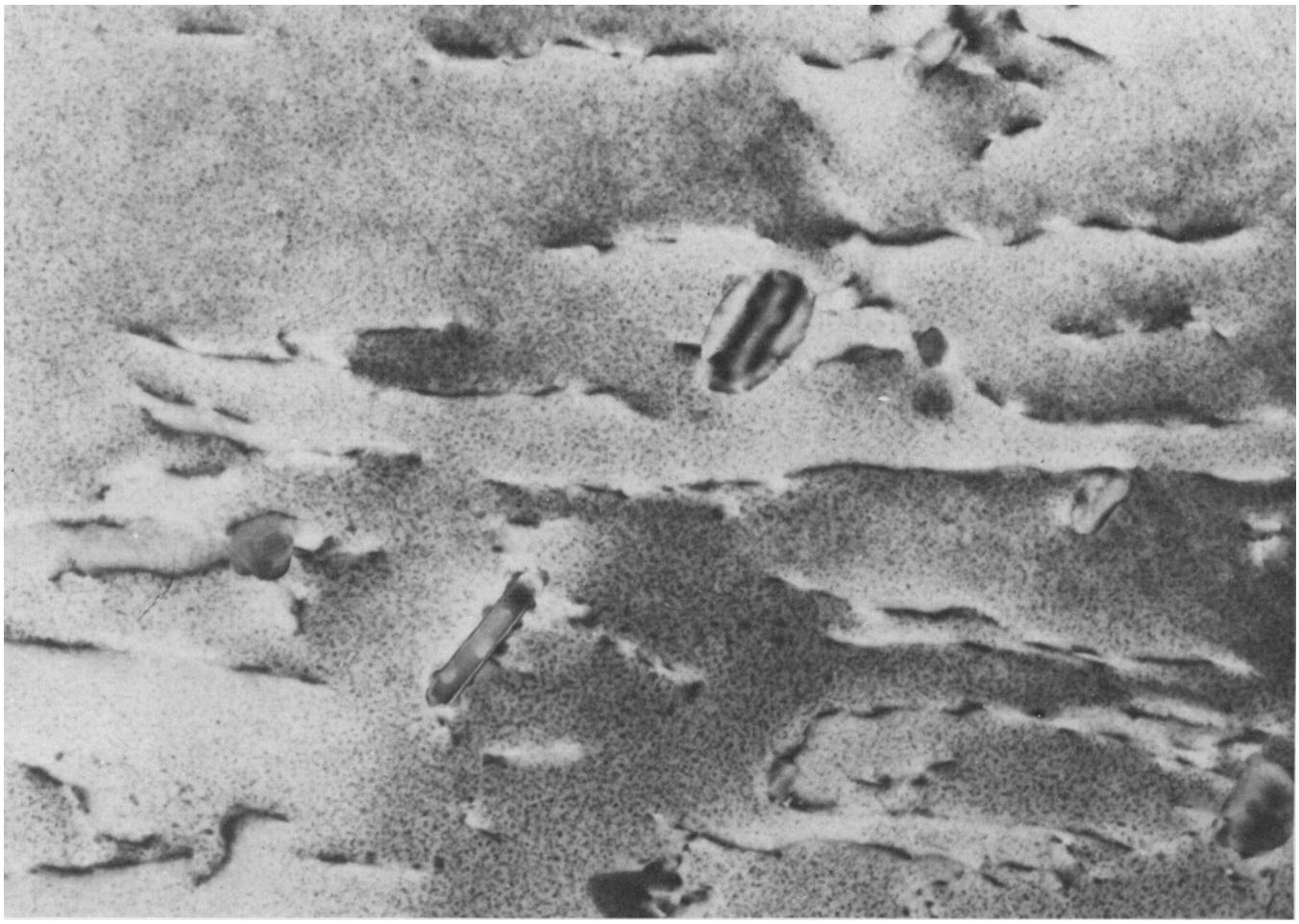

Fig. 3—Transmission electron micrograph of commercial aluminum alloy C7075T651 showing coarse chromium-containing particles, finely dispersed precipitates, and dislocation distribution. Magnification 100,000 times.

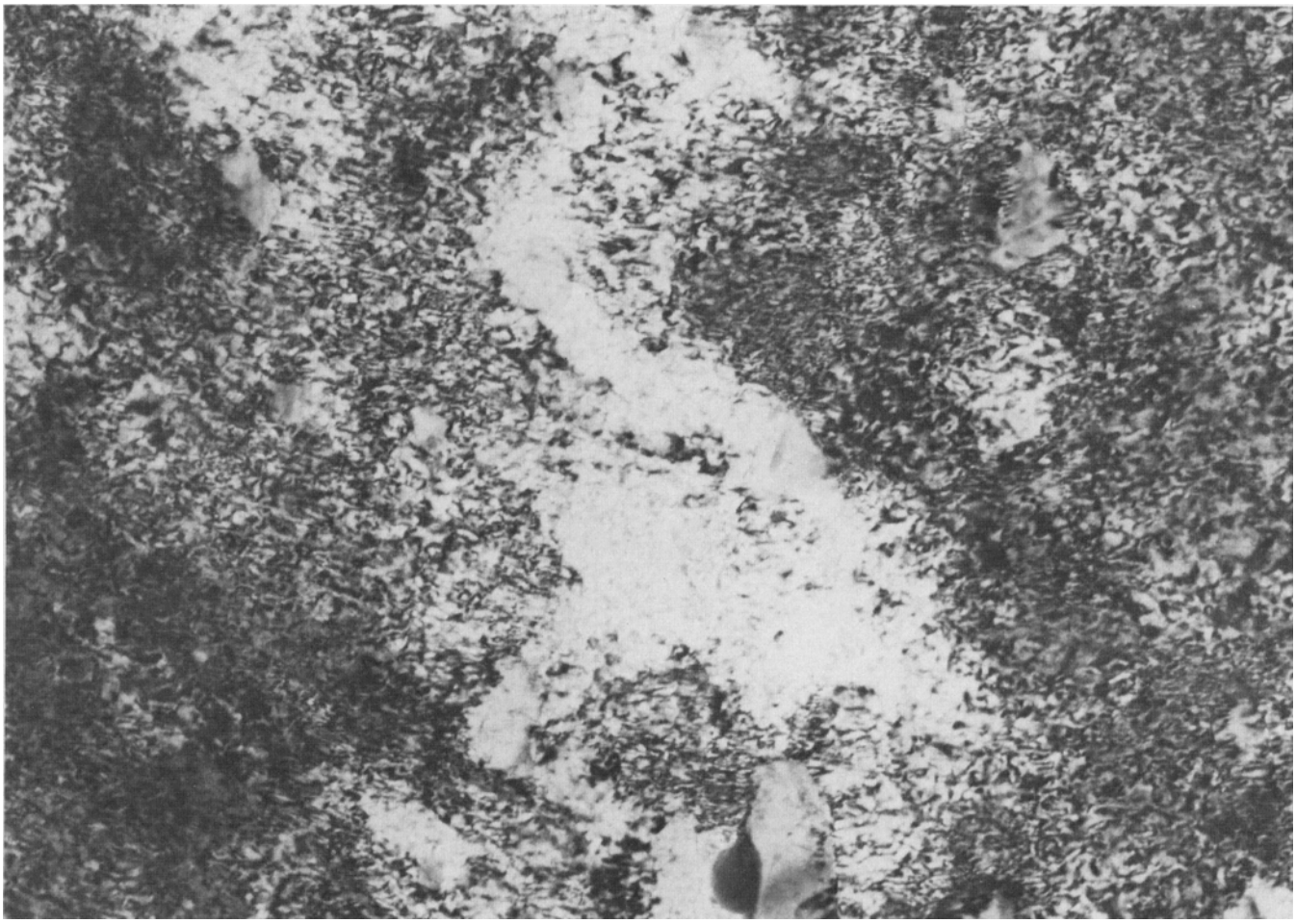

Fig. 4—Transmission electron micrograph of commercial aluminum alloy C7075TMT showing general dislocation distribution. Magnification 100,000 times.

C7075TMT sample, Fig. 1. Coarse intermetallic inclusions in this material were typically arranged in stringers along the bar axis. Individual inclusion sizes ranged around 10 μm and rarely exceeded 20 μm in diameter. The severe etching attack on inclusion particles obscures the fact that many inclusions were cracked transverse to the bar axis in the as-received T651 material. The severe cold swaging did not further accentuate this cracking, which was restricted to the particles only and did not seem to extend into the alloy matrix. The high-purity material contained a much lower volume fraction of inclusions, but their sizes were similar to those of the commercial material. Shape and size range of inclusions in X7075TMT are illustrated in Fig. 2, although the average density of inclusions was much less than that depicted in this figure.

Transmission electron micrographs of the three materials in Figs. 3 to 5 show a more dramatic difference in structure between the TMT and the T651 conditions. The latter treatment introduces a low density of dislocations (by the stretching operation), Fig. 3, whereas the TMT treatment produces a dense dislocation structure without clear evidence of cell formation, although periodic lattice rotations of a few degrees were found within grains, Figs. 4 and 5. The different amounts of cold work in the two TMT conditions have caused a difference in general dislocation density rather than a more or less distinct arrangement of dislocations into cell walls.

The precipitate structure in the T651 condition is evident from Fig. 3 and consists of two types of particles. The coarse particles, measuring approximately 1000Å in at least one dimension, most likely represent a chromium-containing intermetallic phase.[22] These particles do not contribute to strength directly, but seem to interact strongly with dislocations. Their existence does not depend on the presence of iron and silicon, since they were found in similar sizes and numbers also in the high-purity material. The high strength of Al-Zn-Mg-Cu alloys is caused by the exceedingly fine and uniformly dispersed η' phase. In the T651 condition the η' particles appear to have a diameter of 50 to 100Å according to Fig. 3. Because of the high density of dislocations, the fine η' particles are difficult to observe in the TMT conditions except for some regions in Fig. 5 showing small particles of similar size and number as in Fig. 3. The dark field image of X7075TMT in Fig. 6 shows that many small precipitate particles are associated with dislocations. The growth of η' on dislocations and subgrain boundaries has been observed in Al-Zn-Mg alloys by a num-

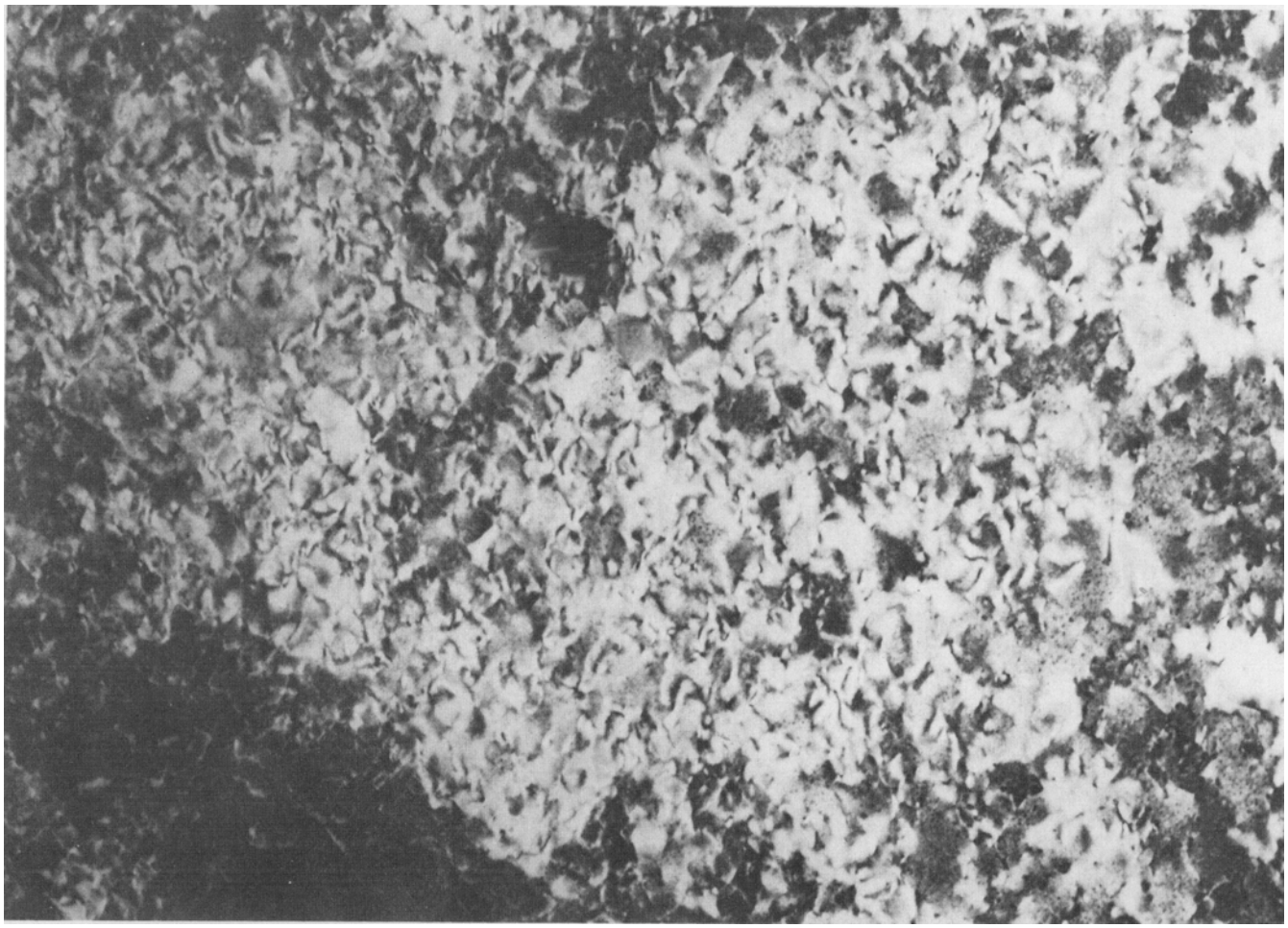

Fig. 5—Transmission electron micrograph of high-purity aluminum alloy X7075TMT showing general dislocation distribution. Magnification 100,000 times.

ber of investigators.[23-27] However, the aging temperatures were commonly higher than used for the present thermomechanical treatment of 7075.

TENSILE PROPERTIES

The tensile properties of the three materials are listed in Table II. Thermomechanical treatments of the commercial and the high-purity alloys have significantly increased the strength without a negative effect on the RA values.* The measured elongation values, however, appear to be sensitive to the amount of cold work introduced during the thermomechanical treatments. Initial portions of true stress-true strain curves are reproduced in Fig. 7. While the conventional 0.2 pct yield strength varies widely between TMT and T651 specimens, the proportional limits of all three materials are almost identical. Beyond the conventional yield strain the work-hardening curves are almost parallel. A careful examination reveals that the work-hardening constants calculated using the simple parabolic work-hardening equation $\sigma = K\epsilon_p^n$ increase as a function of plastic strain for all three materials as indicated in Table III. Also listed in Table III are values of fracture strength calculated from measured rupture loads and reduction-in-area data. It is seen that the values of K calculated from stress-strain data around $\epsilon_p = 0.05$ agree rather well with measured values of fracture strength, although

*The slightly smaller RA value of C7075TMT is only due to the lower uniform elongation, as may be shown by simple computation.

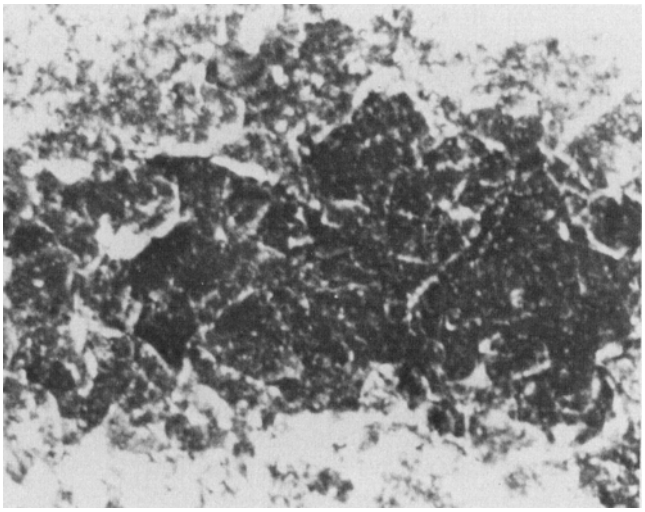

Fig. 6—Transmission electron micrograph of high-purity aluminum alloy X7075TMT. Dark field image shows association of precipitates with dislocations. Magnification 168,000 times.

Table II. Tensile Properties*

Material	0.2 Pct Yield Strength, Ksi	Ultimate Tensile Strength, Ksi	Elongation in 1 in., Pct†	Reduction in Area, Pct
C7075T651	74.9	83.1	16.5 (13)	32
C7075TMT	87.2	91.0	10.0 (8)	29
X7075TMT	85.3	91.8	12.7 (8)	34

*Average of two tests; specimen gage dimensions: 1 in. long and 0.25 in. diam.
†Numbers in parentheses are uniform elongation values.

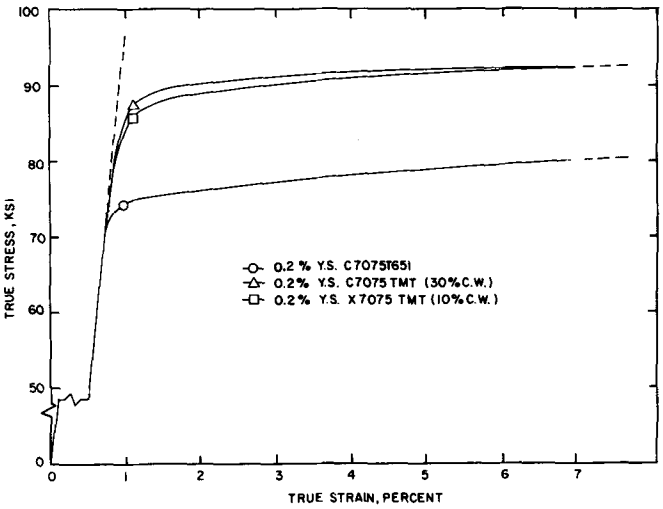

Fig. 7—Initial portions of true stress-true strain curves of high-purity and commercial 7075 in T651 and TMT conditions.

the latter have not been corrected for the triaxial state of stress in the necked region.

FATIGUE PROPERTIES

Axial load fatigue tests were conducted in a 2-ton Schenck Pulsator at around 2400 rpm and with zero mean load ($R = -1$). Threaded 0.5 in. round, 3 in. long hour-glass specimens (2 in. radius) with 0.2 in. net section diameter were machined and longitudinally polished according to specifications outlined by Lazan and Blatherwick.[28] The experimental data are recorded in the S-N diagram of Fig. 8. Tests in the low stress region were terminated after 20 million load cycles. When compared with the commercial 7075T651 data, thermomechanical treatments of the commercial and high-purity alloys produce significant improvements of fatigue strength. The effectiveness of the thermomechanical treatments applied is most noticeable at long cyclic lives. The alternating stress to cause failure in 10^7 cycles for C7075TMT and X7075TMT is more than 25 pct and almost 50 pct higher, respectively, than for C7075T651. Because of the similar testing conditions Lazan and Blatherwick's[28,29] fatigue results on commercial, rolled and extruded 7075T6 bars are included in Fig. 8 for comparison.

DISCUSSION

The remarkable difference in fatigue resistance between 7075TMT and 7075T651 material obtained from the same commercial bar stock seems to support qualitatively the arguments of Ostermann and Reimann[17] for microstructural control, when high fatigue resistance is desired. It is encouraging to observe the notable influence of submicrostructure despite the presence of intermetallic or nonmetallic inclusion particles, which are thought to have an overriding effect on crack nucleation in age-hardening aluminum alloys. Inclusions in 7075 and 2024 aluminum alloys have been found by Grosskreutz and coworkers[11-13] to be the singular origin of fatigue cracks. Improvements of cyclic life or sustained cyclic stress can be obtained by decreasing the size and volume fraction of intermetallic inclusions in 2024T4.[30-32] Testing commercial and homogenized 7075T6 materials Mulherin and Rosenthal,[33] however, found improved fatigue resistance only in short transverse grain direction. On the other hand, the data on commercial and high-purity 7075TMT in Fig. 8 indicate a substantial longitudinal fatigue strength improvement at lives in the range of 10^7 cycles.

Another indirect indication for a beneficial effect of thermomechanical processing on the prevailing fatigue mechanisms of 7075 aluminum can be derived from a change in endurance ratio (ratio of endurance strength to ultimate tensile strength) among the various experimental materials of Fig. 8. While this ratio is approximately 0.22 for T6 or T651 material, it increases to 0.27 or higher for TMT material. It is interesting that the static strength and fatigue data of 7075T6 extrusions tested by Lazan and Blatherwick[29] should both be similar to those of the TMT material tested here. This coincidence is perhaps evidence for a more general,

Table III. Constants of Parabolic Work-Hardening at Two Levels of Plastic Strain ($\sigma = K\epsilon_p^n$)

Material	ϵ_p	n	K, Ksi	σ_f, Ksi*
C7075T651	0.003	0.015	82.4	
	0.050	0.099	113.5	113.4
C7075TMT	0.002	0.037	110.5	
	0.050	0.056	115.4	117.7
X7075TMT	0.003	0.025	101.4	
	0.050	0.073	121.3	124.9

*Fracture strength calculated from rupture load and reduction-in-area values but not corrected for stress state in the necked region.

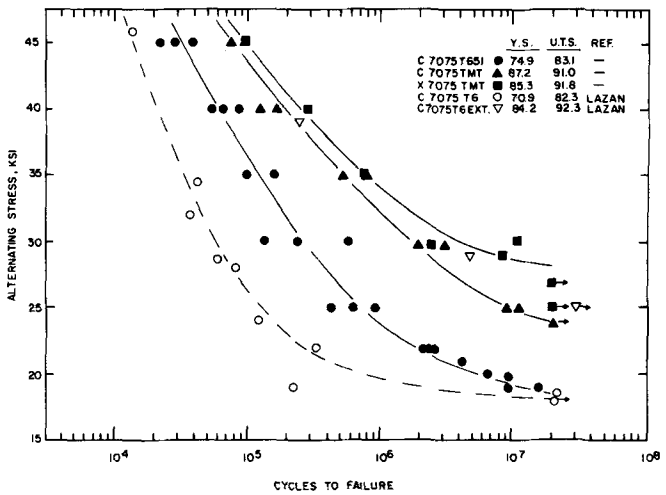

Fig. 8—S-N curves of 7075 aluminum alloys with and without thermomechanical treatments. Axial loading with $R = -1$.

beneficial influence of dislocation substructures on tensile and fatigue strength of 7075 aluminum, and directs attention to other types of thermomechanical treatments, particularly to those which can be applied during primary processing.

Cold-working often produces microstructural instabilities under fatigue loading. The phenomenological interrelations between static and cyclic stress-strain properties have provided a useful framework,[34] within which some deductions about the microstructural stability of thermomechanically treated aluminum alloys can be made. Because of the high stacking fault energy age-hardened aluminum alloys should deform in a wavy slip mode, although the straight and narrow surface slip topography gives the impression of planar slip mode. A characteristic feature of wavy slip materials is the existence of a unique cyclic stress-strain curve, irrespective of work-hardened or annealed microstructural conditions. This has been recently shown by Laird and Krause[16] to be the case also for cold-worked and aged Al-Mg alloys. The overall cyclic strain-softening of work-hardened wavy glide materials will be minor at long cyclic lives and low stresses. However, softening can occur in localized small areas such as deformation bands,[35] the total effect being localized strain accumulation with a detrimental influence on life and endurance strength. The increase in fatigue strength due to cold work will consequently be small compared to the increase in ultimate tensile strength.[16,34]

The cyclic stress-strain behavior of 7075T6 rolled bar stock was investigated by Endo and Morrow.[36] The static and cyclic work-hardening exponents were nearly equal ($n = n' = 0.11$) and the material showed cyclic strain-hardening in the T6 condition. The fair agreement between the static strength and work-hardening properties of C7075T651 in Table III and those obtained by Endo and Morrow suggests similar cyclic stress-strain behavior for the C7075T651 material described here. With the fracture strength being roughly equal, the lower strain hardening exponents of the alloys in TMT condition, see Table III, would indicate the possibility of cyclic strain-softening of the overall structure or in localized regions. Following the above reasoning of Feltner and Beadmore[34] a reduced endurance ratio should result from localized cyclic softening which, however, is contrary to the observed increase of endurance ratio for TMT material. Therefore, while direct evidence is missing, it must be assumed that the particular TMT microstructures illustrated in Figs. 4 to 6 are stable enough to resist localized cyclic softening.

The higher endurance ratio of the TMT material implies that the static strength increase is not the only reason for the different fatigue behavior. The mechanism by which the TMT process improves the fatigue strength needs much further study, but a possible explanation may be derived from the tensile behavior illustrated in Fig. 7 and Table III. At plastic strains below 0.002 TMT material strain-hardens much more rapidly than the T651 material. The deformation of TMT samples should be correspondingly more homogeneous, which is expected to reduce strain concentrations (*e.g.* at inclusions), to retard the formation of fatigue crack nuclei, and hence to increase the fatigue resistance at long lives.

CONCLUSIONS

A thermomechanical treatment has been shown to improve the fatigue strength of 7075 aluminum. The uniform dislocation-precipitate structure appears to be stable and to resist localized cyclic strain softening. The evidence strongly suggests that the dislocation-precipitate structure is as important for fatigue resistance of commercial alloys as controlling the size and volume fraction of intermetallic and nonmetallic inclusions.

ACKNOWLEDGMENT

The author is indebted to his colleagues at AFML and at the Metallurgy and Ceramics Research Laboratory of ARL for many helpful discussions and active participation in performing this investigation, and to Walter J. Trapp, Chief of Strength and Dynamics Branch, for the original stimulus and his enthusiastic support.

REFERENCES

1. P. J. E. Forsyth: *Proc. of the Crack Propagation Symposium, Cranfield, 1961,* pp. 76-94, College of Aeronautics, Cranfield, 1962.
2. P. J. E. Forsyth: *Acta Met,* 1963, vol. 11, pp. 703-715.
3. P. J. E. Forsyth: *J. Australian Inst. Metals,* 1963, vol. 8, pp. 52-60.
4. A. J. McEvily, Jr., J. B. Clark, E. C. Utley, and W. H. Herrnstein, III: *Trans. TMS-AIME,* 1963, vol. 227, pp. 1093-97.
5. J. B. Clark and A. J. McEvily: *Acta Met,* 1964, vol. 12, pp. 1359-72.
6. A. J. McEvily, Jr., J. B. Clark, and A. P. Bond: *Trans. ASM,* 1967, vol. 60, pp. 661-71.
7. T. Broom, J. A. Mazza, and V. N. Whittaker: *J. Inst. Metals,* 1957-58, vol. 86, pp. 17.
8. I. J. Polmear and I. F. Bainbridge: *Phil. Mag.,* 1959, vol. 4, pp. 1293-1304.
9. C. A. Stubbington and P. J. E. Forsyth: *Acta Met.,* 1966, vol. 14, pp. 5-12.
10. A. Abel and R. K. Ham: *Acta Met,* 1966, vol. 14, pp. 1495-1503.
11. J. C. Grosskreutz and G. G. Shaw: *Mechanisms of Fatigue in 7075-T6 Aluminum,* AFML-TR-66-96, May 1966, AD 486 769.
12. J. C. Grosskreutz and G. G. Shaw: *Critical Mechanisms in the Development of Fatigue Cracks in 2024-T4 Aluminum,* AFML-TR-68-137, May 1968, AD 840 403.
13. J. C. Grosskreutz and G. G. Shaw: *Fracture–1969, Proc. Second Intern. Conf. on Fracture,* Brighton, April 1969, P. L. Pratt, ed., p. 620, Chapman and Hall, Ltd.
14. C. Laird and G. Thomas: *Intern. J. Fracture Mech.,* 1967, vol. 3, pp. 81-97.
15. A. R. Krause and C. Laird: *Mater. Sci. Eng.,* 1967-68, vol. 2, pp. 331-47.
16. C. Laird and A. R. Krause, *Inelastic Behavior of Solids,* M. F. Kanninen, W. F. Adler, A. R. Rosenfield, and R. I. Jaffee, eds., pp. 691-715, McGraw-Hill Book Co., New York, 1970.
17. F. G. Ostermann and W. H. Reimann: *ASTM Spec. Tech. Publ.* 467, Am. Soc. Testing Mater., 1970, pp. 169-87.
18. G. Thomas and J. Nutting: *J. Inst. Metals,* 1957-58, vol. 86, pp. 7-14.
19. M. O. Speidel: *Fundamental Aspects of Stress Corrosion Cracking,* pp. 561-79, National Association of Corrosion Engineers, Texas, 1969.
20. A. J. Jacobs: *Fundamental Aspects of Stress Corrosion Cracking,* pp. 530-57, National Association of Corrosion Engineers, Texas, 1969.
21. F. Ostermann and A. W. Brisbane: unpublished research, 1970.
22. H. A. Holl: *J. Inst. Metals,* 1969, vol. 97, pp. 200-05.
23. R. B. Nicholson, G. Thomas and J. Nutting: *J. Inst. Metals,* 1958-59, vol. 87, pp. 429-38.
24. G. Thomas and J. Nutting: *J. Inst. Metals,* 1959-60, vol. 88, pp. 81-90.
25. G. Thomas: *Phil. Mag.,* 1959, vol. 4, pp. 606-11.
26. H. A. Holl: *J. Inst. Metals,* 1964-65, vol. 93, pp. 364-65.
27. H. A. Holl: *Metal Sci. J.,* 1967, vol. 1, pp. 111-18.
28. B. J. Lazan and A. A. Blatherwick: WADC-TR-52-307, Pt. I, 1953, AD 7610.
29. B. J. Lazan and A. A. Blatherwick: WADC-TR-52-307, Pt. II, 1952, AD 8136.
30. P. Brenner: *Aluminum,* 1956, vol. 32, pp. 756-68.
31. J. C. Grosskreutz, G. G. Shaw, and D. K. Benson: *The Effect of Inclusion Size and Distribution on Fatigue of 2024-T4 Aluminum,* AFML-TR-69-121, 1969, AD 856 763.
32. F. Ostermann: unpublished research, 1971.
33. J. H. Mulherin and H. Rosenthal: *Met. Trans.,* 1971, vol. 2, pp. 427-32.
34. C. E. Feltner and P. Beadmore: *ASTM Spec. Tech. Publ.* 467, Am. Soc. Testing Mater., 1970, pp. 77-112.
35. C. E. Feltner: unpublished research, cited in Ref. 16.
36. T. Endo and JoDean Morrow: *J. Mater.,* 1969, vol. 4, pp. 159-75.